

Anderson transition in systems with chiral symmetry

Antonio M. García-García

*Physics Department, Princeton University, Princeton, New Jersey 08544, USA and
The Abdus Salam International Centre for Theoretical Physics, P. O. Box 586, 34100 Trieste, Italy*

Emilio Cuevas

Departamento de Física, Universidad de Murcia, E30071 Murcia, Spain

(Dated: March 23, 2024)

Anderson localization is a universal quantum feature caused by destructive interference. On the other hand chiral symmetry is a key ingredient in different problems of theoretical physics: from nonperturbative QCD to highly doped semiconductors. We investigate the interplay of these two phenomena in the context of a three-dimensional disordered system. We show that chiral symmetry induces an Anderson transition (AT) in the region close to the band center. Typical properties at the AT such as multifractality and critical statistics are quantitatively affected by this additional symmetry. The origin of the AT has been traced back to the power-law decay of the eigenstates; this feature may also be relevant in systems without chiral symmetry.

PACS numbers: 72.15.Rn, 05.40.-a, 05.45.Df, 71.30.+h

The combination of global symmetries and dimensionality provides us with a useful classification scheme for the study of Anderson localization.¹ According to the one-parameter scaling theory (ST),² all eigenstates of a disordered system are exponentially localized in fewer than two dimensions in the thermodynamic limit and undergo a localization-delocalization transition [or Anderson transition (AT)] in higher dimensions, if the strength of disorder is sufficiently weak. However, deviations from ST predictions have been found in systems with additional discrete symmetries. A typical example is a disordered lattice without on-site disorder but random hopping amplitudes.³ Formally, the system may be considered as two independent sublattices with nonzero matrix elements connecting only sites of different sublattices. The corresponding Hamiltonian is invariant under a simultaneous sign flip of an arbitrary eigenvalue and the eigenstate components of one of the associated sublattices. As a consequence of this discrete symmetry, referred to as chiral symmetry, eigenvalues of the Hamiltonian come in pairs of $\pm\epsilon$, that is, the spectrum is invariant around the point $\epsilon = 0$. This symmetry is an important ingredient in different problems of theoretical physics: from the QCD Dirac operator⁴ to bosons in random media⁵ and the spectrum of a highly doped semiconductor.⁶

From the definition of chiral symmetry it is clear that one must distinguish between eigenvalues near zero (the origin) and distant from it (the bulk). In the bulk, spectral correlations in the metallic limit are described by the universal results of random matrix theory (RMT), usually referred to as Wigner-Dyson (WD) statistics.⁷ Weak-localization corrections to these universal results are obtained by mapping the localization problem onto a supersymmetric nonlinear σ model.⁸ The transition to localization occurring for stronger disorder is beyond the reach of current analytical techniques. Numerical results suggest that the AT is characterized by multifractal⁹ eigenfunctions, a scale-invariant spectrum,¹⁰ and spectral correlations (usually referred to as "critical statistics"¹¹) different from Poisson and WD statistics.^{10,12} These properties are supposed to be universal, namely, they do not depend on the microscopic details of the Hamiltonian but only on the dimensionality and symmetries of the system.

sionality and symmetries of the system.

In contrast, much less is known about the region close to the origin where the chiral symmetry plays a crucial role. An exception is the metallic limit, where the effect of this symmetry on level statistics¹³ has been investigated in detail with the help of the powerful analytical techniques of RMT. Beyond this region we are still far from even a qualitative understanding of the interplay between disorder and chiral symmetry. As a general rule, chiral symmetry tends to delocalize eigenstates close to the origin since weak-localization corrections vanish.¹⁴ Indeed in the one-dimensional case it can be rigorously proved³ that, in disagreement with the ST prediction, eigenstates at the band center are not localized exponentially. In two dimensions, localization properties seem to be very sensitive to the microscopic form of the random potential.¹⁵ For the specific case of a weak Gaussian disorder, it is well established that eigenvectors at the band center remain delocalized.¹⁶ In three-dimensions (3D), for weak disorder and time-reversal invariance, the results of Refs.17,18,19 suggest that chiral symmetry may induce power-law localization of the zero-energy eigenstates.

Surprisingly, with the exception of certain one-dimensional systems with long range disorder,^{20,21} the transition to localization in systems with chiral symmetry has hardly been studied despite its potential applications to the description of the chiral phase transition in QCD,²² or the metal-insulator transition in highly doped semiconductors. The present Brief Report is a step in this direction. We investigate the interplay between chiral symmetry and localization in a three-dimensional system with short-range disorder. Our main finding is that chiral symmetry induces an AT in the region close to the origin. Eigenstates are power-law localized with an exponent that increases as we move from the origin. The AT occurs when this exponent matches the dimensionality of the space. We recall that, since the AT is to a great extent universal, the validity of our results does not depend on the microscopic details of the model but only on the dimensionality of the space and the (chiral) symmetry of the Hamiltonian.

We consider the following 3D tight-binding Hamiltonian

with only off-diagonal disorder:

$$H = \sum_{\langle i,j \rangle} t_{ij} e^{i\phi_{ij}} a_i^\dagger a_j + \text{H.c.}; \quad (1)$$

where the sum is restricted to nearest neighbors and the operator a_i (a_i^\dagger) destroys (creates) an electron at the i th site of the 3D cubic lattice. We break time-reversal invariance by introducing a random magnetic flux described by the above Peierls phase $e^{i\phi_{ij}}$ with ϕ_{ij} uniformly distributed in the interval $[-\pi; \pi]$. Although we mainly focus on the broken time-reversal case, we have also checked that our main conclusions are valid if time-reversal invariance is preserved. The hopping integrals t_{ij} are real random variables satisfying the probability distribution

$$P(\ln t_{ij}) = 1/W \quad \text{for} \quad -W \leq \ln t_{ij} \leq 0; \quad (2)$$

and zero otherwise. The above exponential distribution provides an effective way of setting the strength of off-diagonal disorder.²³

In order to proceed, we compute eigenvalues and eigenvectors of the Hamiltonian (1) for different volumes L^3 by using standard numerical diagonalization techniques. The number of disorder realizations for each volume L^3 ranges from 10^4 ($L = 10$) to 500 ($L = 20$). Hard-wall boundary conditions are imposed in order to better examine the asymptotic decay of eigenstates in real space (see below). Since we are interested in the effect of chiral symmetry we mainly focus on a small energy window close to the origin $\epsilon = 0$. The eigenvalues thus obtained are appropriately unfolded, i.e., they were rescaled so that the spectral density on a spectral window comprising several level spacings is unity.

Our first task is to look for a mobility edge in a small spectral window close to the origin. The chosen interval, $[-2 \times 10^{-4}; 2 \times 10^{-3}]$ in our case, is not important provided that it is close to the origin. For other intervals one gets similar results but for a different critical disorder. We recall that in general the value $W = W_c$ for which the system undergoes an AT is quite sensitive to the details of the Hamiltonian and consequently is not universal. In order to locate the mobility edge we use the finite size scaling method.¹⁰ First we evaluate a certain spectral correlator for different sizes and disorder strengths W . Then we locate the mobility edge by finding the disorder W_c such that the spectral correlator analyzed becomes size independent.¹⁰

In our case we investigate the level spacing distribution $P(s)$ [the probability of finding two neighboring eigenvalues at a distance $s_i = (\epsilon_{i+1} - \epsilon_i)/\bar{\epsilon}$, with $\bar{\epsilon}$ being the local mean level spacing]. The scaling behavior of $P(s)$ is examined through the following function of its variance:²⁴

$$(\bar{L}; W) = [\text{var}(s) / \text{var}_{WD}] / [\text{var}_P / \text{var}_{WD}]; \quad (3)$$

which describes the relative deviation of $\text{var}(s)$ from the WD limit. In Eq. (3) $\text{var}(s) = \overline{(\epsilon_{i+1} - \epsilon_i)^2} / \bar{\epsilon}^2$, where $\bar{\epsilon}$ denotes the AT (critical statistics) combine typical properties of a metal (WD) with those of an insulator (Poisson). Thus level repulsion $P(s) \neq 0$ for $s \neq 0$, typical of WD statistics is still present at the AT. However, a long-range correlator such as the

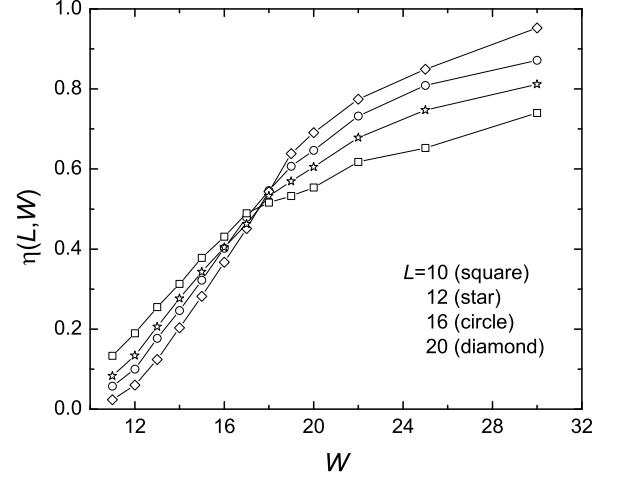


FIG. 1: Scaling variable η as a function of disorder W for different volumes; only eigenvalues in the window 10^{-4} to 10^{-3} have been considered. The system undergoes an AT at $W = W_c \approx 18$. In all cases the statistical error (not shown) is ≈ 0.003 .

other intermediate value of η in the thermodynamic limit is an indication of a mobility edge.

In Fig. 1 we plot the W dependence of η for different system sizes. It is clear that, in the window of energy studied $[-2 \times 10^{-4}; 2 \times 10^{-3}]$, the mobility edge signaling an AT is located around $W_c \approx 18$. We have also found that W_c increases as the energy window of interest gets closer to the origin. For a weaker (stronger) disorder, η tends slowly to the WD (Poisson) results. This slow convergence to WD statistics (see Fig. 1) suggests that eigenstates may still have some kind of structure even on the delocalized side of the transition. The analysis of eigenfunctions will show that this is the case. We have checked that the use of scaling variables other than η do not alter the results. For the sake of completeness we repeat the calculation for the case of time-reversal invariance, $\phi_{ij} = 0$ in Eq. (1). We have also observed a mobility edge with similar properties but at a slightly weaker disorder $W_c \approx 15$, in agreement with previous results for the standard 3D AT.²⁶ Finally, we remark that the study of $\eta(W; L)$ for different disorders and system sizes is equivalent to the standard renormalization group analysis of the dimensionless conductance g . For instance, according to the one-parameter scaling theory, g should be scale invariant at the AT. Any spectral correlator, in particular, is a function of g only and, consequently, it should be scale invariant at the AT as well. We have chosen η instead of g for numerical reasons. The former is easier to calculate and provides much more stable results.

We now study whether level statistics around the mobility edge are compatible with those of an AT. Spectral correlations around the AT (critical statistics) combine typical properties of a metal (WD) with those of an insulator (Poisson). Thus level repulsion $P(s) \neq 0$ for $s \neq 0$, typical of WD statistics is still present at the AT. However, a long-range correlator such as the

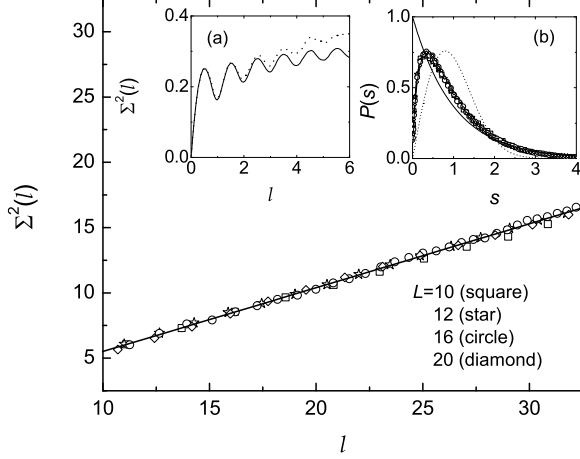


FIG. 2: The $1/l$ behavior of the number variance $\Sigma^2(l)$ and $P(s)$ [inset (b)] in the spectral window $2 (10^{-4}; 10^{-3})$ at the critical point $W_c = 18$ for different volumes. $\Sigma^2(l)$ is linear with a slope (solid line) 0.49 ± 0.01 , $P(s) \sim s^{-1}$ for $s > 1$, and both are size independent. These features are typical signatures of critical statistics. For $W = 0.2 < W_c$ [inset (a)] the number variance (dotted line) is well described by the prediction of chiral RMT (solid line).

the number variance $\Sigma^2(\gamma) = \hbar(N \cdot \hbar N \cdot i)^2 i$ for $\gamma \rightarrow 1$ ($N \cdot$ is the number of eigenvalues in an interval of length γ) is asymptotically linear,¹² as for an insulator $\Sigma^2(\gamma) \sim \gamma$, but with a slope < 1 (0.27 for 3D AT).

As shown in Fig. 2 all these features are also present in our model. However, we have found that the slope of the number variance $= 0.49 \pm 0.01$ is roughly twice that of the standard 3D AT. We refer to the analysis of eigenvectors (see below) for a qualitative explanation of this feature.

We have verified that the number variance in the limit of weak disorder agrees with the prediction¹³ of chiral RMT [see inset (a) Fig. 2]. For weak enough disorder results depend on whether the time-reversal invariance is broken [inset (a) in Fig. 2] or not (not shown). As a general rule, as disorder is increased the magnetic flux gets weaker, for $W \rightarrow 10$ we could not observe any difference. Additionally, we have found that, if chiral symmetry is broken, by for instance adding a weak diagonal disorder, level statistics are very close to the Poisson limit typical of an insulator.

To conclude, the analysis of level statistics shows that, as a consequence of the chiral symmetry of the model, there is an AT close to the band center with properties similar but not equal to those of the standard 3D AT.

One of the signatures of an AT transition is the multifractality of the eigenstates. An eigenfunction is said to be multifractal (for an alternative definition see Ref. 27) if the eigenfunction moments $P_q = \frac{1}{L} \sum_{j=1}^L |\psi_j|^q$ present anomalous scaling with respect to the sample size L , where D_q is a set of different exponents describing the transition.^{28,29}

After performing ensemble and spectral averaging in the

spectral window $2 (10^{-4}; 10^{-3})$ we have found that the eigenfunctions are indeed multifractal ($D_2 = 0.69 \pm 0.02$, $D_3 = 0.45 \pm 0.01$, and $D_4 = 0.340 \pm 0.007$). These values of D_q are, roughly speaking, a factor of 2 smaller than the ones at the standard 3D AT. This is consistent with our results from level statistics, where a similar factor was found for the slope of the number variance $\Sigma^2(\gamma)$. Qualitatively, this numerical difference can be traced back to the chiral symmetry of our model: according to the ST, parameters such as D_q or D_2 are functions of the dimensionless conductance g_c at the AT. Although an explicit expression is not known, it is expected that, at least for sufficiently high dimensions, both D_2 and $1/\Sigma^2(\gamma)$ will be proportional to g_c . On the other hand, it is well established^{14,16} that weak-localization corrections vanish in systems with chiral symmetry. Hence, a stronger disorder is needed to reach the AT region. As a consequence, the chiral g_c will be smaller, in qualitative agreement with our results. Having discussed the details of the AT close to the origin, we now clarify the physical mechanism causing this transition. Chiral systems do not have weak-localization corrections, so the transition to localization must be in part due to some nonperturbative effect, such as tunneling combined with the progressive weakening of the effect of the chiral symmetry as we move away from the origin. On the other hand, the slow rate of convergence toward WD statistics observed in Fig. 1 suggests that, although eigenstates seem to be delocalized in the thermodynamic limit, they still have some kind of localization center. This is in agreement with the results of Ref. 17, where it was found that the zero-energy wave function of a time-reversed, weakly disordered 3D chiral system was power-law localized $\langle r \rangle \sim r^{(W)}$. We recall that, according to Refs. 28 and 30, power-law localization induces an AT in any dimension provided that the decay exponent matches the dimensionality d of the space. If $< (>) d$, eigenstates tend to be delocalized (localized) in the thermodynamic limit but the degree of convergence is slow.³¹

Based on the above facts we claim that the transition to localization close to the origin observed in the Hamiltonian (1) has its origin in the power-law localization of the eigenstates. We remark that this mechanism should be at work for any system with chiral symmetry and disorder such that a mobility edge appears close to the origin. The Hamiltonian (1) was chosen for the sake of simplicity. It is just one of the simplest representatives of the universality class associated with the AT in systems with chiral symmetry.

Moreover, for a given spectral window close to the origin, we expect the exponent describing the decay to increase with the disorder strength W . The AT will occur for a $W = W_c$ so that $d = 3$. For stronger disorder $W > W_c$ eigenstates must be eventually exponentially localized, though they may still possess a power-law tail for distances smaller than the localization length.

We have tested this conjecture by analyzing the typical decay of eigenstates in the window $10^{-4} \dots 10^{-3}$ for $L = 20$ and different W 's (similar results are obtained if W is kept fixed and the energy window is modified) through the following correlation function:³²

$$g(r) = \hbar \ln \left(\frac{1}{L} \sum_{j=1}^L |\psi_j|^2 \right) / \ln \left(\frac{1}{L} \sum_{j=1}^L |\psi_j|^2 \right) ; r = \sum_{j=1}^L |\psi_j|^2 ; \quad (4)$$

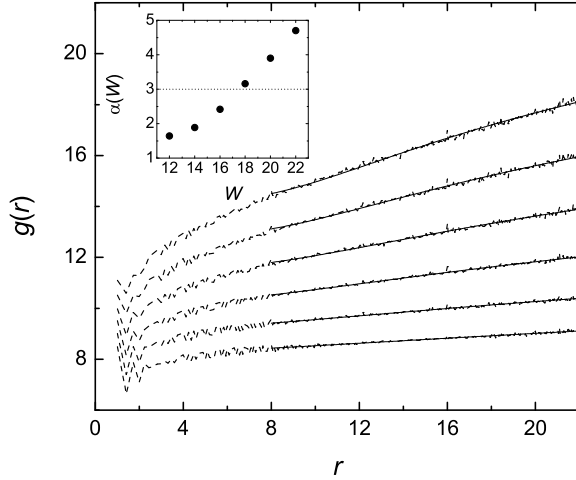


FIG. 3: The correlation function $g(r)$ as a function of r (dashed lines) for a system size $L = 20$ and $W = 12, 14, 16, 18, 20$, and 22 from bottom to top. The numerical curves were fitted to a curve of the form $g(r) = \ln(Ar + B)$ (solid lines). The best-fitting parameter is represented as a function of W in the inset. In all cases the statistical error (not shown) is ≈ 50 .

where j_{max} denotes the lattice site with the largest amplitude and the angular brackets stand for the ensemble average. In order to examine the asymptotic decay of $g(r)$ (we restrict ourselves to the range $8 \leq r \leq 22$), we fit the numerical results to a curve of the form $g(r) = \ln(Ar + B)$ with A , B , and α fitting parameters. The parameters A and B describe finite-size effects and remnants of the eigenstate core (nondecaying) part. The exponent α (depicted in the inset of Fig. 3) provides us with valuable information about the decay of the eigenstates.

The excellent agreement (see Fig. 3) between the numerical results and the fitting curve indicates that eigenstates are power-law localized. Moreover, the exponent α controlling

the decay increases with W and tends to the conjectured value $\alpha = 3$ as we get close to the critical disorder $W_c \approx 18$. Thus chiral symmetry combined with strong disorder induces power-law localization and eventually an AT close to the origin. This is the most relevant result of the paper.

We remark that the relation between chiral symmetry and power-law localization has already been established in the context of QCD (see Ref. 18 and references therein). Specifically, it was found that the low-lying eigenstates of the QCD operator (with gauge configurations given by the instanton liquid model) are power-law localized due to the long-range behavior of certain nonperturbative solutions (instantons) of the classical equations of motion. We speculate that a similar mechanism is at work in our case.

A final comment is in order: the claim that the power-law localization is the precursor of the AT is not in contradiction with the multifractal structure of the eigenstates. Since $g(r)$ is averaged over many realization of disorder, all multifractal fluctuations are washed out. What remains is the smooth skeleton of the eigenstate which, in our case, has a power-law tail.

To conclude, we have investigated the interplay between chiral symmetry and Anderson localization in a 3D Anderson model with off-diagonal disorder. Close to the origin we have found a mobility edge induced by the chiral symmetry with properties quantitatively different from those of a standard 3D AT. This chiral AT can be traced back to the power-law nature of eigenstates close to the origin. Our results are relevant to chiral systems undergoing a metal-insulator transition as a function of disorder. Typical examples include the QCD Dirac operator around the chiral phase transition and highly doped semiconductors where off-diagonal bond disorder plays a dominant role.

A.M.G. acknowledges support from the European Union, Marie Curie program, Contract No. MOIF-CT-2005-007300. E.C. thanks the FEDER and the Spanish DGI for financial support through Project No. FIS2004-03117.

- ¹ P. W. Anderson, Phys. Rev. **109**, 1492 (1958).
- ² E. Abrahams *et al.* Phys. Rev. Lett. **42**, 673 (1979).
- ³ F. J. Dyson, Phys. Rev. **92**, 1331 (1953).
- ⁴ E. V. Shuryak *et al.*, Nucl. Phys. A **560**, 306 (1993).
- ⁵ V. Gurarie and J. T. Chalker, Phys. Rev. Lett. **89**, 136801 (2002).
- ⁶ B. I. Shklovskii and A. L. Efros, *Electronic Properties of Doped Semiconductors* (Springer-Verlag, Berlin, 1984).
- ⁷ E. P. Wigner, Ann. Math. **53**, 36 (1951); F. J. Dyson, J. Math. Phys. **3**, 140 (1962); **3**, 157 (1962); **3**, 166 (1962).
- ⁸ K. B. Efetov, Adv. Phys. **32**, 53 (1983).
- ⁹ M. Schreiber and H. Grussbach, Phys. Rev. Lett. **67**, 607 (1991); H. Aoki, J. Phys. C **16**, L205 (1983).
- ¹⁰ B. I. Shklovskii *et al.*, Phys. Rev. B **47**, 11487 (1993).
- ¹¹ V. E. Kravtsov and K. A. Muttalib, Phys. Rev. Lett. **79**, 1913 (1997); S. M. Nishigaki, Phys. Rev. E **59**, 2853 (1999).
- ¹² B. L. Altshuler *et al.*, Zh. Eksp. Teor. Fiz. **94**, 343 (1988) [Sov. Phys. JETP **67**, 625 (1988)].
- ¹³ P. J. Forrester, Nucl. Phys. B **553**, 601 (1999); T. Nagao, J. Math. Phys. **34**, 2317 (1993); J. Verbaarschot, Phys. Rev. Lett. **72**, 2531 (1994); K. Slevin and T. Nagao, *ibid.* **70**, 635 (1993); A. Altland and M. R. Zirnbauer, Phys. Rev. B **55**, 1142 (1997).
- ¹⁴ C. Mudry, P. W. Brouwer, and A. Furusaki, Phys. Rev. B **62**, 8249 (2000); E. Louis and J. A. Vergés, *ibid.* **63**, 115310 (2001).
- ¹⁵ W. A. Atkinson *et al.*, Phys. Rev. Lett. **85**, 3926 (2000).
- ¹⁶ R. Gade, Nucl. Phys. B **398**, 499 (1993); A. Furusaki, Phys. Rev. Lett. **82**, 604 (1999); K. Takahashi and S. Iida, Phys. Rev. B **63**, 214201 (2001); V. Z. Cerovski, *ibid.* **62**, 12775 (2000).
- ¹⁷ S. J. Xiong and S. N. Evangelou, Phys. Rev. B **64**, 113107 (2001).
- ¹⁸ A. M. García-García *et al.*, Phys. Rev. Lett. **93**, 132002 (2004).
- ¹⁹ B. K. Nikolic, Phys. Rev. B **64**, 014203 (2001).
- ²⁰ A. M. García-García and K. Takahashi, Nucl. Phys. B **700**, 361 (2004); D. A. Parshin and H.R. Schober, Phys. Rev. B **57**, 10232

- (1998).
- ²¹ A. M. García-García *et al.*, Nucl. Phys. B **586**, 668 (2000).
 - ²² A. M. García-García *et al.*, Nucl. Phys. A **770**, 141 (2006).
 - ²³ B. Huckenstein, Rev. Mod. Phys. **67**, 357 (1995); S. N. Evangelou, J. Phys. C **19**, 4291 (1986).
 - ²⁴ E. Cuevas, Phys. Rev. Lett. **83**, 140 (1999); E. Cuevas, E. Louis, and J. A. Vergés, *ibid.* **77**, 1970 (1996).
 - ²⁵ J. Pipek and I. Varga, Phys. Rev. A **46**, 3148 (1992).
 - ²⁶ E. Hofstetter and M. Schreiber, Phys. Rev. Lett. **73**, 3137 (1994).
 - ²⁷ E. Cuevas, Phys. Rev. B **68**, 024206 (2003).
 - ²⁸ A. D. Mirlin, Phys. Rep. **326**, 259 (2000).
 - ²⁹ F. Wegner, Z. Phys. B **36**, 209 (1980).
 - ³⁰ L. S. Levitov, Phys. Rev. Lett. **64**, 547 (1990).
 - ³¹ A. D. Mirlin *et al.*, Phys. Rev. E **54**, 3221 (1996); F. Evers and A. D. Mirlin, Phys. Rev. Lett. **84**, 3690 (2000); E. Cuevas *et al.*, *ibid.* **88**, 016401 (2002).
 - ³² M. Inui *et al.*, Phys. Rev. B **49**, 3190 (1994).